Understanding the nature of metal-graphene contacts: a theoretical and experimental study

Teresa Cusati[a], Gianluca Fiori[a], Amit Gahoi[c], Vikram Passi[c], Alessandro Fortunelli[b], Max Lemme[c], Giuseppe Iannaccone[a*]

[a)]University of Pisa, Pisa, Italy; [b)]CNR-ICCOM, Pisa, Italy;[c)]University of Siegen, Germany

*email:giuseppe.iannaccone@unipi.it

Abstract

In this paper we propose a theoretical and experimental study of the nature of metal-graphene contacts. We use ab-initio simulations and semi-analytical modeling to derive and validate a simple two-parameter model of metal-graphene contacts. Such findings are supported by experimental results for large samples of different types of metal-graphene contacts.

Motivation

The quality of metal contacts is a critical aspect for the performance of transistors and other devices and sensors using two-dimensional materials. For example, a low contact resistance (≤100 Ωμm) is required for high-performance graphene-based transistors, as it impacts the device f_{MAX} for analog and radio-frequency applications, and the propagation delay of digital gates (1). An in-depth understanding of the physics of graphene-metal contacts is required to be able to control and engineering them, as experimental and theoretical studies provide a broad range of contact resistances for the same metals (2-11), due to limited reproducibility of contact fabrication technology and incomplete consideration of influencing factors.

Here we present a theoretical and experimental study of metal-graphene contacts for different metals, and we propose and validate a physical model on the basis of ab-initio simulations and experiments. We can also predict a minimum achievable contact resistance well below 100 Ωμm.

Approach

We have performed ab-initio calculations with Quantum Espresso (12) of the symmetric structures shown in Fig. 1, using a plane-wave basis set and a gradient-corrected exchange-correlation functional (Perdew-Burke-Ernzerhof)(13). We have considered four different metals, divided in two categories, based on the binding energy and the metal-graphene distance: chemisorbed metals (Ni, Pd), with stronger bonds and physisorbed metals (Cu, Pt), with weaker bonds (Fig. 2).

We have then cut the region in one of the points indicated in Fig. 1, and have attached a semi-infinite metal lead on the left, and a semi-infinite graphene lead on the right. We have then computed the transmission coefficient via the solution of the scattering problem considering incoming and outgoing Bloch states as implemented in the

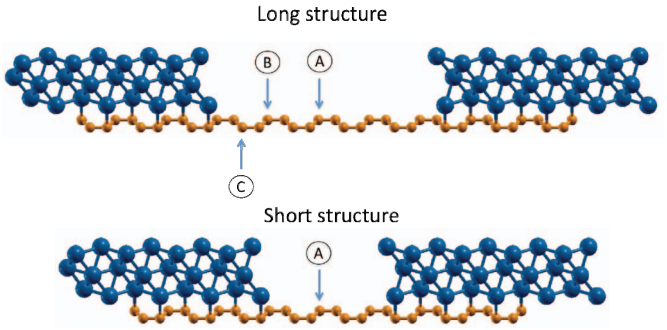

Figure 1. Simulated structures with ab-initio simulations, including two metallic (nickel) regions connected by one graphene region of different length. Simmetric structures ensure that no artifact dipoles appear. Transport is computed with PWCOND by cutting the structure at one of the "points" indicated, and by attaching semi-infinite metal and graphene leads.

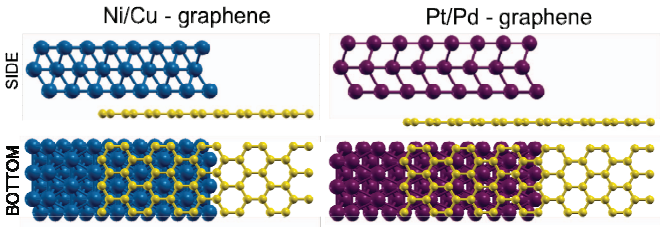

Figure 2. Side and bottom views of the scattering regions considered for the density-functional theory and transmission calculations, for the Ni-, Cu-, Pt- and Pd-graphene contacts.

PWCOND module of Quantum Espresso (14). The transmission coefficient strongly depends on the cut point (Fig. 3). This means that the "free" (i.e. non contacted) graphene region has a strong impact on contact resistance, both in ballistic transport calculations and in experiments, where it is not usually taken into account.

For each type of contact we have extracted the energy of the Dirac point at the interface (15) relative to the Fermi energy (indicated with $\Delta E_{F\text{-}cont}$ in Fig. 4). Graphene Dirac point energy moves $\Delta E_{F\text{-}cont}$ to the Fermi Energy as one moves from the contact to the center, because graphene is undoped and the electric field is progressively screened. As we expect, the absolute value of the Dirac point energy in the point of

symmetry (Points "A" of Fig. 1) is larger for the short structure (SS) than for the long structure (LS). Indeed, this is verified by considering in Fig. 5 the plot of the transmission coefficient as a function of energy for all four metallic contacts and for the short and long structures (the cut point in graphene is the point of symmetry). As expected, the energy at which the transmission coefficient is zero is larger (in absolute value) in SS than in LS. Such energy corresponds to the energy of the cut point in graphene (where the semi-infinite graphene lead is applied).

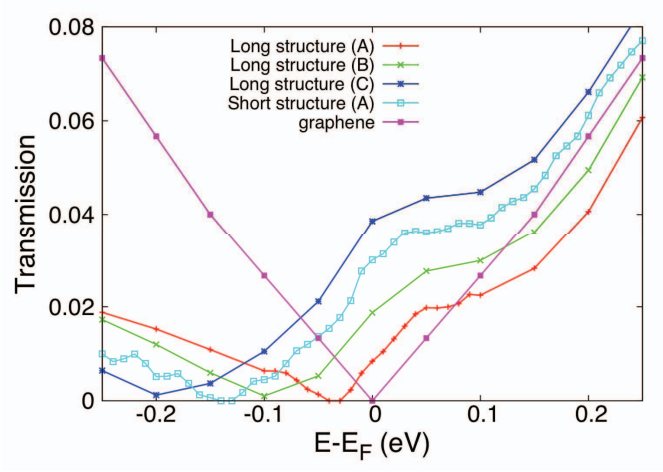

Figure 3. Transmission coefficient as a function of energy computed for nickel-graphene contacts for different cutting points, corresponding to those indicated in Fig. 1. It is clear that the transmission coefficient and the conductance strongly depend on the cut point.

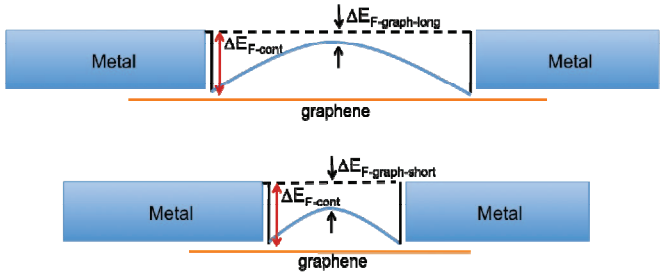

Figure 4. Profile of the Dirac point in graphene between metal regions.

As a consequence, contact resistance computed with Landauer's formula is very different for the long structure and for the short structure (Table 1). A correspondingly wide variation is observed in experiments and in theoretical literature results, because the contact resistance depends on the energy of the Dirac point (i.e. on the charge density) in the graphene layer, *which is often not controlled in the literature.* In the case of palladium, the discrepancy is due to a considered contact interface that does not correspond to the experimental one.

Let us stress here that the length scale at which the Dirac point energy changes is very small (1-2 nm from the metal surface), therefore four-probe or transfer-length methods cannot correct for this effect. It is an uncontrolled factor, up to now, but very important: even in the case of ballistic transport, graphene resistance per unit width depends on Dirac point energy, reaching a maximum of about 310 Ωμm (Fig. 6).

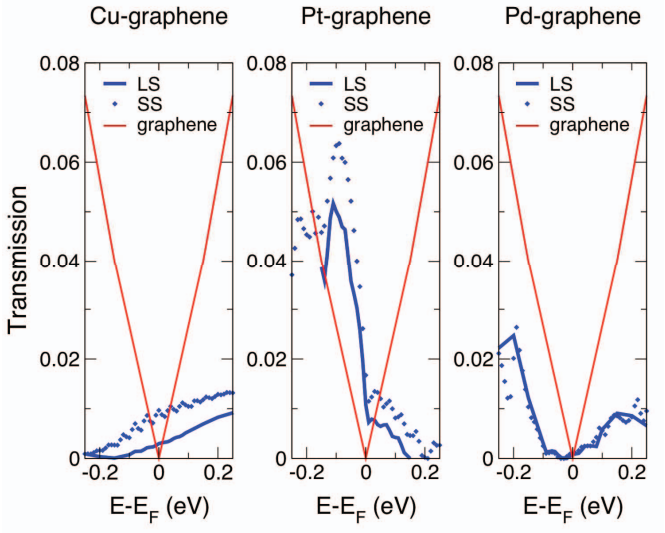

Figure 5: Transmission for metal-graphene systems obtained with PWCOND for different metals (Cu,Ni,Pd,Pt) compared with the transmission of the ideal graphene monolayer, for the short structure (SS) and for the long structure (LS). As can be seen, the energy at which transmission is zero is typically larger (in absolute value) for the short system, since in the undoped graphene the Dirac point tends to get closer to the Fermi energy as one moves away from the contacts.

Table 1: Resistance per unit width for different metal contacts in the case of the LS, the SS, available literature on experiments and theory. Data for palladium-graphene contacts are very far from the literature. Our interpretation is that for Pd-graphene we consider a contact interface that is rather different from the experimental one.

Metal	Long structure (Ωμ·m)	Short structure (Ωμ·m)	Experimental results from literature (Ωμ·m)	Theoretical results from literature (Ωμ·m)
Cu	1096	374		627 (5) 44 (3)
Ni	333	120	294 (2) 300 (6) 800 (8) 170-260 (11)	600 (4)
Pd	2291	2076	320-715 (10) 600 (6) 170-250 (7)	403 (5) 584 (9)
Pt	175	123		764 (2)

Indeed, we can see (Table 2), that the ratio of the ballistic resistance of graphene in the semi-infinite lead (i.e. at the cut point) to the contact resistance only depends on the type of metal, not on the distance between the two metal regions. We can therefore interpret it as an effective

transmission coefficient of the contact at the Fermi energy (T). This means that we have a simple physical model of the contact - even simpler than that described in Ref. (11) - based on only two parameters that can be extracted with ab-initio simulations: T and $\Delta E_{F\text{-cont.}}$ It also allows us to predict that the *measured contact resistance (e.g. obtained using the transfer-length method) must be proportional to the graphene sheet resistance.*

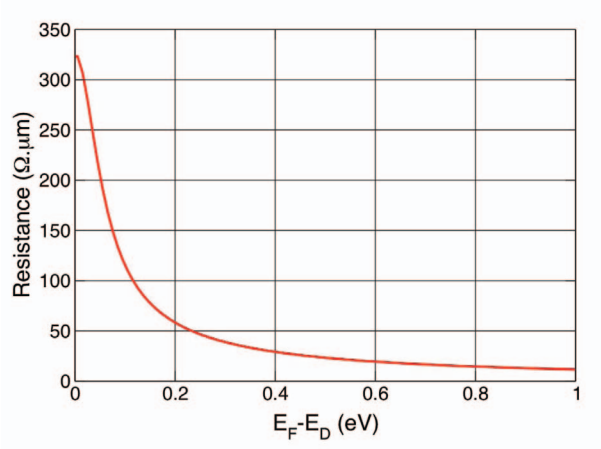

Figure 6: Resistance of graphene per unit width in the case of ballistic transport as a function of the position of the Dirac point with respect to the Fermi energy. Directly computed from the graphene bandstructure.

Table2: Resistance ballistic graphene in the semi-infinite lead applied to the symmetry point of the structure (Graphene R) and resistance of the metal-graphene contacts (Total R) for different metals structure length. As can be seen, the ratio of the two (Ratio) is almost independent of the length of the structure.

	Short structure				Long structure			
	Total R (Ωμ·m)	$E_F - E_D$ (eV)	Graphene R (Ωμ·m)	Ratio Teff	Total R (Ωμ·m)	$E_F - E_D$ (eV)	Graphene R (Ωμ·m)	Ratio Teff
Cu	374	-0.336	46.6	0.12	1153	-0.166	70.6	0.06
Ni	120	-0.136	83	0.69	360	-0.036	245	0.74
Pd	2076	-0.036	230	0.11	2899	-0.025	273	0.12
Pt	123	0.209	58.3	0.47	209	0.155	77	0.44

Experiments

We have performed experiments on different metal-graphene contacts, considering different distances between metal electrodes (Fig. 7). All the structures have a back gate, that allows us to tune the energy of the Dirac point. Metals include Ni (thickness 75 nm), Ni-Au (25/50 nm), Au (75 nm), Pt-Au (25/50 nm). The contact and sheet resistances are extracted for each contact and as a function of the back gate voltage with the transfer-length method (Fig. 8). In Fig. 9 we plot, for each type of contact resistance as a function of the sheet resistance of graphene, obtained for different back gate bias. As can be seen, the correlation between the two quantities is very high (R>0.96), validating our interpretation and our proposed model.

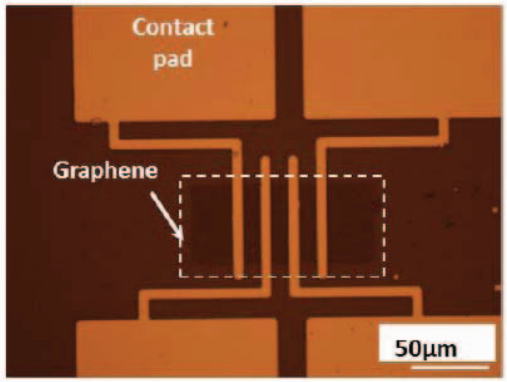

Figure 7: Photograph of one of the structures used for the measurements of metal-graphene contact resistances with the transfer-length methods.

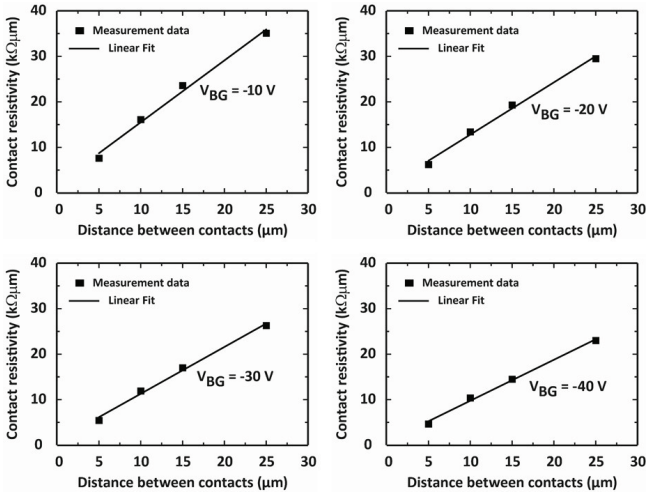

Figure 8: Experiments: extraction of the contact resistance and of the sheet resistance with the transfer-length method for different backgate voltages in the case of nickel-graphene contacts. The same procedure is repeated for gold, nickel-gold, and platinum-gold contacts.

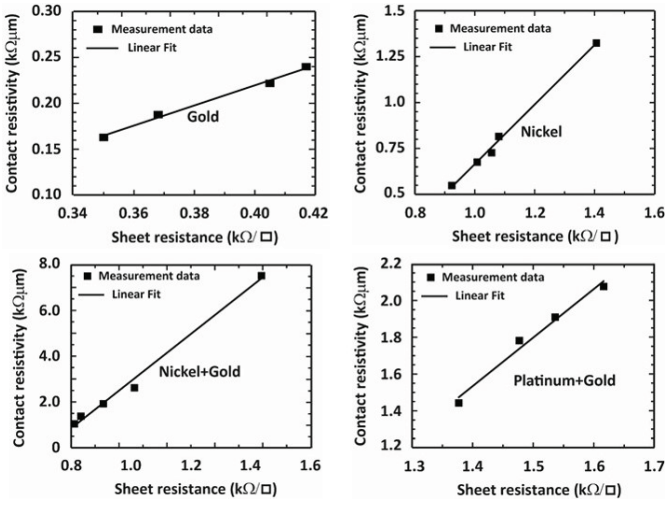

Figure 9: Experiments: Correlation between the contact resistance and the graphene sheet resistance for four different metal-graphene contacts. In all cases correlation is very high (R>0.96) , confirming our interpretation.

Concluding remarks

Through ab-initio simulations and experiments we have improved our understanding of metal-graphene contacts, and have derived and validated a synthetic model to be used in device-level simulations based on only two parameters: an effective contact transmission coefficient T and the Dirac point energy at the contact $\Delta E_{F\text{-cont}}$ (Fig. 10b). Contact optimization requires us to adjust the Dirac point of graphene in the contact region with a back gate (Fig. 10a) or with adequate doping. In order to obtain the minimum achievable contact resistance we need to put the system in the condition illustrated in Fig. 10c, i.e. with flat potential in the graphene layer in the contact region, so that we have minimum sheet resistance of graphene close to the contact. When this happens, as shown in Table 3, we have the minimum contact resistance achievable for a given metal. Indeed, contact resistance can be as low as 30 Ωμm for nickel contacts, which would be very desirable for high performance graphene-based FETs (2,16,17). Further investigation is required to properly capture in the models the chemistry of the palladium-graphene interface.

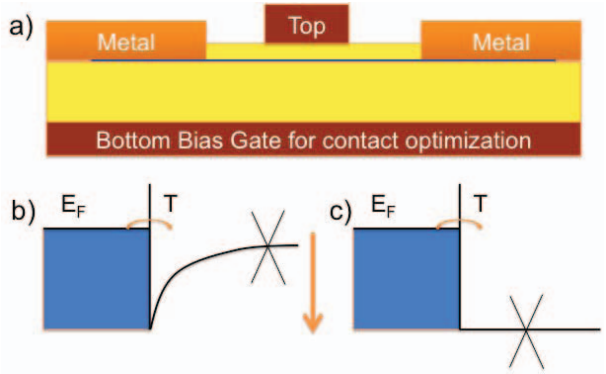

Figure 10: (a) FET device structure with back gate. (b) illustration of the simple model of metal-graphene contact c) condition of minimum contact resistance, obtained by properly adjusting the graphene Dirac point near the contacts.

Table 3: Minimum achievable contact resistance for different metals if the situation illustrated in Fig. 10c is obtained. We have considered the T and $E_{F\_cont} = E_F - E_D$ extracted from ab-initio simulations.

Metal	$E_F - E_D$ (eV) Interface	T interface	Minimum graphene R (ballistic) (Ωμ·m)	Contact asymptotic R (ballistic) (Ωμ·m)
Cu	-0.503 (n-type)	0.08	23.5	294
Ni	-0.559 (n-type)	0.69	21	30.5
Pd	-0.171 (n-type)	0.09	68	755
Pt	0.218 (p-type)	0.36	54	150

Acknowledgements

This work was supported in part by the EC 7FP through the Project GRADE (contract n. 317839), the Project GO-NEXTS (contract n. 309201), and the Graphene Flagship (contract 604391).

References

(1) Z. Chen, and J. Appenzeller, "Gate modulation of graphene contacts on the scaling of graphene fets," *VLSI Symp. Tech Dig. VLSI Japan*, vol. 13, pp. 128-129, June 2009.
(2) W.S. Leong, H. Gong, and J.T.L. Thong, "Low-contact-resistance graphene devices with nickel-etched-graphene contacts," *ACS Nano*, vol 8, pp. 994-1001, January 2014.
(3) J. Maassen, W. Ji, and H. Guo, "First princuples study of electronic transport through a Cu(111)-graphene junction," *Appl. Phys. Lett.*, vol. 97, pp. 142105, October 2010.
(4) K. Stokbro, M. Engelund, and A. Blom, "Atomic-scale model for the contact resistance of the nickel-graphene interface," *Phys. Rev. B*, vol. 85, pp. 165442, April 2012.
(5) X. Ji, J. Zhang, Y. Wang, H. Quian, and Z. Yu, "A theoretical model for the contact resistance using a DFT-NEGF method," *Phys. Chem. Chem. Phys.*, vol. 15, pp. 17883-17886, November 2013.
(6) E. Watanabe, A. Conwill, D. Tsuya, and Y. Koide, "Low contact resistance metals for graphene based devices," *Diamond & Rel. Mat.*, vol 24, pp. 171-174, April 2012.
(7) F. Xia, V. Perebeinos, Y.M. Lin, Y. Wu, and P. Avouris, "The origins and limits of metal-graphene junction resistance," *Nat. Nanotechnology*, vol 6, pp. 179-184, March 2011.
(8) K. Nagashio, T. Nishimura, K. Kita, and A. Toriumi, "Contact resistivity and current flow path at metal/graphene contact," *Appl. Phys. Lett.*, vol. 97, pp. 143514, October 2010.
(9) J.T. Smith, A.D. Franklin, D.B. Farmer, and C.D. Dimitrakopoulos, "Reducing contact resistance in graphene devices through contact area patterning," *ACS Nano*, vol. 7, pp. 3661-3667, April 2013.
(10) A.D. Franklin, S.-J. Han, A.A. Bol, and V. Perebeinos, "Double contacts for improved performance of graphene transistors." *IEEE Elec. Device Lett.*, vol 33, pp. 17-19, January 2012.
(11) F.A. Chaves, D. Jiménez, A.A. Sagade, W. Kim, J. Riikonen, H. Lipsanen, and D. Neumaier, "A physics-based model of gate-tunable metal-graphene contact resistance benchmarked against experimental data," *2D Materials*, vol. 2, pp. 025006, June 2015.
(12) P. Giannozzi et al, "QUANTUM ESPRESSO: a modular and open source software project for quantum simulations of materials," *J. Phys.: Condens. Matter*, vol. 21, pp. 395502, September 2009.
(13) J.P. Perdew, K. Burke, and M. Ernzerhof, "Generalized gradient approximation made simple," Phys. Rev. Lett., vol 77, pp. 3865-3868, October 1996.
(14) A. Smogunov, A. Dal Corso, and E. Tosatti, "Ballistic conductance of magnetic Co and Ni nanowires with ultrasoft pseudopotentials," *Phys. Rev. B*, vol 70, pp. 045417, July 2004.
(15) A. Franciosi, and C. G. Van de Walle, "Heterojunction band offset engineering", Surf. Sci. Rep. 25, 1-140, 1996.
(16) G. Fiori, D. Neumaier, B. N. Szafranek, G. Iannaccone, "Bilayer Graphene Transistors for Analog Electronics", *IEEE Trans. Electron Devices* Vol. 61, n. 3, pp. 729-733, March 2014.
(17) M. Cheli, G. Fiori, G. Iannaccone, "A Semianalytical Model of Bilayer-Graphene Field-Effect Transistor", *IEEE Transactions on Electron Devices*, Vol. 56, pp.12979-2986, December 2009.